

Two conformational states of Glu242 and pK_a s in bovine cytochrome *c* oxidase†‡§

Dragan M. Popovic and Alexei A. Stuchebrukhov*

Received 4th January 2006, Accepted 30th March 2006

First published as an Advance Article on the web 20th April 2006

DOI: 10.1039/b600096g

Cytochrome *c* oxidase (CcO) is the terminal enzyme in the respiratory electron transport chain of aerobic organisms. It catalyses the reduction of atmospheric oxygen to water, and couples this reaction to proton pumping across the membrane; this process generates the electrochemical gradient that subsequently drives the synthesis of ATP. The molecular details of the mechanism by which electron transfer is coupled to proton pumping in CcO is poorly understood. Recent calculations from our group indicate that His291, a ligand of the Cu_B center of the enzyme, may play the role of the pumping element. In this paper we describe calculations in which a DFT/continuum electrostatic method is used to explore the coupling of the conformational changes of Glu242 residue, the main proton donor of both chemical and pump protons, to its pK_a , and the pK_a of His291, a putative proton loading site of our pumping model. The computations are done for several redox states of metal centers, different protonation states of Glu242 and His291, and two well-defined conformations of the Glu242 side chain. Thus, in addition to equilibrium redox/protonation states of the catalytic cycle, we also examine the transient and intermediate states. Different dielectric models are employed to investigate the robustness of the results, and their viability in the light of the proposed proton pumping mechanism of CcO. The main results are in agreement with the experimental measurements and support the proposed pumping mechanism. Additionally, the present calculations indicate a possibility of gating through conformational changes of Glu242; namely, in the pumping step, we find that Glu242 needs to be reprotonated before His291 can eject a proton to the P-site of membrane. As a result, the reprotonation of Glu can control proton release from the proton loading site.

1. Introduction

Cytochrome *c* oxidase (CcO) is the terminal enzyme in the electron transport chain of aerobic organisms, which catalyses the reduction of molecular oxygen to water, and utilizes the free energy of the redox reaction to pump protons across the membrane, a process that creates the proton gradient which subsequently drives the synthesis of ATP. In the past decade, a great deal of data has become available on the structure and function of CcO, however, the

molecular mechanism by which electron transfer (ET) is coupled to proton pumping in this enzyme still remains poorly understood.^{1–14}

In our recent studies,^{15–20} we used continuum electrostatic and quantum mechanical calculations to investigate the possibility of a novel mechanism of proton pumping in CcO in which the His291 ligand of the Cu_B center of the enzyme plays the central role. The key element of the model is that upon ET to the binuclear Fe_{a3} – Cu_B catalytic center (BNC) of the enzyme, His291 gets protonated by a proton from Glu242, an established proton donor for both chemical and pumped protons, and the subsequent proton transfer of a chemical proton to the binuclear catalytic center, due to Coulomb repulsion, drives the ejection of the pump proton from His291 to the positive side of the membrane. Thus, His291 plays the role of the proton loading site of the pump. The model involves kinetic gating, which requires that the rate of proton transfer from Glu242 to His291 ought to be greater than the rate between Glu242 and the OH^- group in the catalytic center. This mechanism is referred to as a *Coulomb pump with kinetic gating*.¹⁶

The two key residues of the proposed mechanism are His291 and Glu242. While solid experimental proof for the involvement of His291 in the proton pumping is still lacking, the role of Glu242 residue as a donor of both chemical and pump protons is very well established.^{7,9,21,22} Because of the specific nature of His291 site as a ligand to the Cu_B complex, and the related difficulties of experimentally accessing this residue without perturbing the

Department of Chemistry, University of California, One Shields Avenue, Davis, California, 95616, USA. E-mail: stuchebr@chem.ucdavis.edu, dpopovic@ucdavis.edu; Fax: 530-752-8995; Tel: 530-752-7778

† This paper was published as part of the special issue on Proton Transfer in Biological Systems.

‡ Electronic supplementary information (ESI) available: The influence of the redox state of heme *a* and Cu_B and protonation state of His291 on the pK_a of Glu242 when $\epsilon_{\text{prot}} = 4$ and $\epsilon_{\text{cavity}} = 15$, $\epsilon_{\text{prot}} = 4$ and $\epsilon_{\text{cavity}} = 80$ or $\epsilon_{\text{prot}} = 20$ and $\epsilon_{\text{cavity}} = 20$ (Fig. S1A–C); and the influence of the redox state of heme *a* and Cu_B and the protonation/conformation state of Glu242 on the pK_a of His291 for three different dielectric conditions (Fig. S2). See DOI: 10.1039/b600096g

§ Abbreviations: BNC, binuclear center (complex); CcO, cytochrome *c* oxidase; DFT, density functional theory; E° , redox potential; ET, electron transfer; QM, quantum mechanical; PLS, proton loading site; PRA (PRD), heme propionate A (or D); PRA_{a3} , propionate A of heme *a*₃; PRD_{a3} , propionate D of heme *a*₃; PT, proton transfer; SCRF, self-consistent reaction field. The numbering refers to bovine CcO.

enzyme function, there is very little direct experimental data on His291. In contrast, the Glu242 site has been well characterized, its pK_a has been estimated, and its role in proton translocation has been revealed in mutagenesis studies.^{23,24}

As revealed by computational studies,^{25–27} Glu242 is connected both to propionate D of heme a_3 , and to BNC by two chains of water molecules. Presumably, one water chain leading to propionate D can be used by the pumped protons to load the His291 site located nearby, and the other to transfer chemical protons to BNC, for the reduction of oxygen.

Two possible conformations of Glu242 have been identified and described in the literature:^{28,29} one is to receive a proton from the D-channel, and the other is to release it either along the pumping path, or the chemical path to BNC. The MD simulations show significant conformational freedom of Glu242, so that it can easily switch between the two conformations.

The two conformations of Glu, which will be the subject of this paper, are shown in Fig. 1A. One is a proton input (down) conformation with the Glu side chain pointing downwards; the other, (up) conformation, is a proton releasing one with the Glu side chain pointing upwards. In our calculations, the upper conformation of Glu242 residue is quantum-chemically optimized, and forms a stable hydrogen bond chain between Glu and propionate D with the three intermediate water molecules in between, see Fig. 1B. An additional water molecule is found between PRD a_3 and His291 residue,^{23,30,31} providing an optimal H-bonded chain that may facilitate the proton transfer from Glu242 to the putative proton loading His291 site.

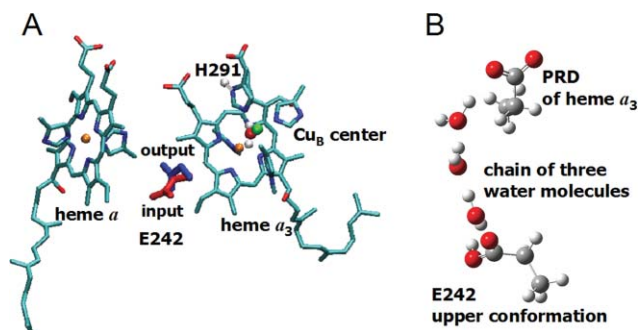


Fig. 1 The two conformations of Glu242 side chain studied in this paper. The heme a , heme a_3 , and Cu_B center are displayed together with three coordinated His residues and a ligated water molecule. Only the position of the H δ 1 proton on His291 residue, which may work as a proton loading site, is explicitly shown. The coordinates of the downward (red) conformation are taken from the X-ray structure of bovine heart cytochrome c oxidase;³³ in this state Glu242 is in contact with the D-channel. The upper (blue) conformation is obtained by an *ab initio* computation of a system consisting of the Glu242 side chain, propionate group (representing PRD of heme a_3) and three water molecules in between, forming a stable H-bonded chain (Fig. 1B; see text for the computational details). The upper conformation is presumably the proton releasing conformation of Glu242 residue.

Experimental evidence showing that Glu242 side chain thermally fluctuates and may adopt one of the two distinct conformations is provided by the crystal structures of wild type and E242Q mutant at pH 10,³² in which these two conformations (*input* and *output*) have been captured. In the mutant structure the side chain of Gln242 points downwards, which is similar to Glu242 in

wild type at pH 7. However, at pH 10, glutamic acid Glu242 is presumably deprotonated and its side chain points upwards.

In the X-ray structures,^{23,30,31,33} the Glu242 residue is found to be in its downward conformation, which is energetically somewhat more stable. However, dynamically the Glu side chain performs thermal fluctuations, and whenever a proton needs to be passed to the BNC for the chemical reaction or to the proton loading site, the protonated Glu side chain presumably goes up into its upward conformation to form the stable H-bonded water chain with the proton acceptor group. Of course, as always, the energetics will decide if the proton transfer is thermodynamically feasible between the proton-donor Glu242 residue and the proton-acceptor group. For a proton transfer to occur, the pK_a of the His proton loading site (or oxygen ligand to the BNC) needs to be higher than the pK_a of Glu242 in its upper conformation.²⁰

In a recent work, the functional intermediate E, R_2 , P_m , F and O states of the catalytic cycle in CcO have been examined by IR difference spectroscopy.³⁴ The study suggests deprotonation of the glutamic acid Glu242 in the E and P_m states. The work of several other groups, on the other hand, based on the measurements of the pH-dependent proton transfer (PT) rates and FTIR spectroscopy, shows that Glu242 has an equilibrium $pK_a \geq 9$,^{35–40} and should be protonated, at equilibrium, at pH 7. Still, the equilibrium value of pK_a does not preclude Glu242 from losing a proton during the catalytic cycle to another group, *e.g.* His291, as in our model. These experimental data has motivated us to investigate the possible dependence of pK_a of His291 and Glu242 on the conformational changes of Glu side chain.

In this paper, we report the results of calculations that combine DFT and continuum electrostatics to examine the coupling of the conformational changes of Glu242 side chain to the pK_a values of the two key residues of the model, Glu242 and His291. A number of different states have been investigated in order to gain insights into the proton pumping mechanism of CcO. In addition to different equilibrium redox/protonation states of the catalytic cycle, we also examine some of the non-equilibrium states. The effects of the coupling of the redox states of the metal centers and protonation states of Glu242 and His291 are evaluated. Different dielectric models are employed to investigate the robustness of the results, to compare results with available experimental data, and to estimate their feasibility in the pumping mechanism.

2. Method and models

2.1 DFT/electrostatic method

The calculations of the pK_a values of His291 and Glu242 have been done using a method that combines DFT (Jaguar 5.5 program⁴¹) and continuum electrostatic calculations (MEAD suite,⁴² and Karlsberg program⁴³), as described in our recent work.¹⁹

Briefly, in the calculations the whole system is divided into a quantum mechanical (QM) part, and the surrounding medium, which consists of the rest of the protein, membrane, internal cavities and external aqueous phase. The membrane was modeled as a low dielectric region of 45 Å thickness that covers the *trans*-membrane helices of the subunit A and B. Density functional theory⁴⁴ is applied to a relatively small QM system, to optimize its geometry, evaluate the gas phase electronic energies (E_{elec}), calculate the reorganization energies (G_{strain}), and obtain the ESP atomic

partial charges for the different redox and protonation states of the complex. Electrostatic calculations, on the other hand, are used to evaluate the reaction (G_{Born}) and protein field (G_q) solvation energies. The $\text{p}K_a$ of the active site complex in protein can be obtained relative to the $\text{p}K_a$ of the appropriate model compound in aqueous solution,[¶] according to the following expression

$$\text{p}K_a^{\text{site}} = \text{p}K_a^{\text{model}} + \frac{(\Delta\Delta E_{\text{elec}} + \Delta\Delta G_{\text{strain}} + \Delta\Delta G_{\text{Born}} + \Delta\Delta G_q)}{kT \ln 10} \quad (1)$$

where double difference is due to the difference in energy between deprotonated and protonated forms, and the energy shift relative to the model compound.¹⁹ The protein charges (and protein field), used in eqn 1, correspond to the equilibrium protonation state of the enzyme at pH 7, for a given redox state of metal centers. Therefore, the calculated $\text{p}K_a$ of the site matches up with the protonation energy of the site in the protein at pH 7.

The QM model used to calculate the His291 $\text{p}K_a$ consists of the Cu_B center together with the ligated water molecule and three coordinated methylimidazoles (representing His240,* His290 and His291). When the $\text{p}K_a$ of Glu242 was evaluated, only propionic acid representing Glu242 side chain was treated by DFT. The hybrid density functional B3LYP⁴⁵ and open shell electronic configurations (for oxidized Cu_B) are used with a restricted open shell variant of DFT. Geometry optimizations are done with the LACVP+* basis set, while the single point energies are calculated with the LACV3P+* basis set.^{41,46} The non-relativistic electron core potential is included for the Cu atom. The basis sets include polarization and diffuse functions for all heavy atoms. Electronic reorganization of the solute and the corresponding set of the ESP fitted charges for the QM system are obtained by the DFT-SCRF method,⁴⁷ which surrounds the complex by a continuum dielectric. For a detailed set up of the calculations, we refer the reader to our recent publications,^{17,19,20} while a review of the combined DFT/electrostatic method can be found elsewhere.^{48–53}

2.2 Optimization of Glu in upward conformation

Two distinct conformations of the Glu242 side chain, displayed in Fig. 1A, were used in the calculations. The two conformations are: a proton loading (*input*) downward conformation, and a proton releasing (*output*) upward conformation. The downward conformation is taken from the crystal structure of bovine CcO,³³ while the upward conformation is obtained by a quantum chemical optimization of the system shown in Fig. 1B.

The geometry optimization of the structure (the QM system) consisting of the Glu242 side chain, a propionate group (representing $\text{PRD}a_3$) and three intermediate water molecules forming a stable H-bonded chain was performed at the Hartree–Fock level using the 6-31+G* basis set.^{54–57} The $C\alpha$ atoms of the propionic acid (Glu242) and propionate ($\text{PRD}a_3$) were kept frozen in their initial positions, as reported in the crystal structure.³³ The calculation was done in the external protein field of the fixed atomic point charges, and in the presence of the Lennard-Jones potential, which defines the walls of the cavity of the QM system.

¶ The $\text{p}K_a$ of His291 is calculated relative to the $\text{p}K_a$ of methylimidazole in aqueous phase. For the $\text{p}K_a$ of Glu242, propionic acid is used as a model compound.

* Tyr244 cross-linked to His240 is included as a part of QM system.

Table 1 The shortest distances between the O δ atom of carboxylate group of Glu242 side chain (in the two conformations) and nearby metal centers (heme a , heme a_3 , Cu_B) or several important protonatable sites (His291, propionates of heme a_3)

Distance ^a	Conformation	
	Glu242 down	Glu242 up
heme a (Fe)–Glu242(O δ)	13.8	11.5
heme a_3 (Fe)–Glu242(O δ)	12.8	9.7
His291(N δ 1)–Glu242(O δ)	12.7	9.4
Cu_B (Cu)–Glu242(O δ)	11.8	9.0
$\text{PRD}a_3$ (O2 δ)–Glu242(O δ)	11.6	8.0
$\text{PRA}a_3$ (O2 δ)–Glu242(O δ)	16.5	12.8

^a The distances (in Å) are measured between the corresponding heavy atoms denoted in the brackets.

The aim of this optimization was only to get the coordinates of the upward position of the Glu242 side chain, in which Glu is connected to a proton-acceptor group by a stable H-bonded water chain. However, the explicit water molecules of the QM system were not used in the subsequent solvation electrostatic calculations; instead, they were replaced with a continuum dielectric medium which represents the internal protein cavities.

The obtained upward and downward conformations are compared in Table 1.

2.3 Pumping model

In the proposed model,¹⁶ the mechanics of the pumping is similar for all four pumped protons of the enzyme cycle. The states of interest for this paper are shown in Fig. 2. According to the model, the sequence of steps of one pumping event can be described as beginning with the transfer of a chemical proton from Glu242 to the binuclear center that converts OH^- to a water molecule (1).

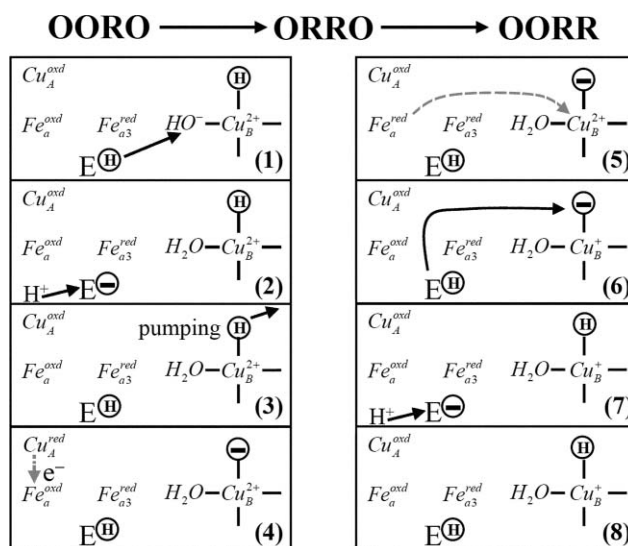
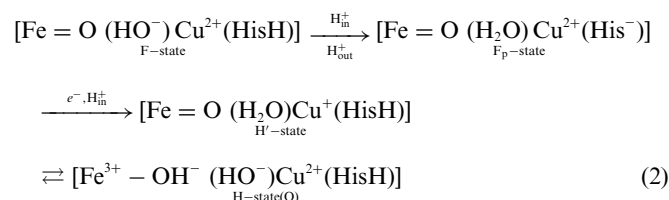


Fig. 2 The schematics of the proposed proton-pumping mechanism of CcO. The sequence of transitions during one pumping cycle of the enzyme is shown. The redox state of Cu_A , heme a , heme a_3 and Cu_B center, and the protonation state of $\text{OH}^-/\text{H}_2\text{O}$ ligand to Cu_B , His291 and Glu242 sites are displayed. Grey dashed arrows represent the ET, while the proton translocations are designated by solid black arrows.

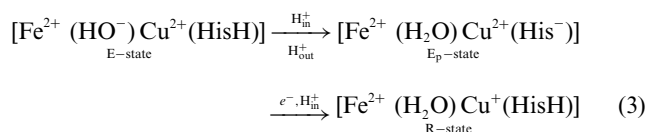
The formed state is formally denoted as OORO redox state.^{††} In the next step Glu242 gets reprotonated (2), and the proton from His291 is expelled (3). In the following steps, an electron is transferred from the *outside* (via cytochrome *c*) first to Cu_A, and then to heme *a* center (4), generating ORRO state. Upon the ET from heme *a* to Cu_B complex (5), a coupled proton transfer from Glu242 to His291 occurs (6). Thus, the proton loading site His291 becomes protonated, generating the OORR state. Finally, Glu242 gets reprotonated once again (7), and the final state of one pumping event is reached (8).

To summarize the notation, the second and third boxes represent the OORO redox state, the fourth box the –RORO state, the fifth box represents the ORRO state, while the sixth to eighth boxes represent the OORR state. In this work, all these redox states have been investigated. In addition, within each redox state (*i.e.* each box in Fig. 2) all possible combinations with respect to protonation state of His291, and the protonation and conformation state of Glu242 have been investigated.

To make it specific, with the steps described, one can think that we are considering the F to H (or O) transition in the catalytic cycle, which in our notation will look like this:



Similarly, the steps in Fig. 2 may be considered as representing transition from E to R:



3. Results and discussion

The dielectric properties of proteins are poorly understood. In order to evaluate the dependence of the results on the dielectric model of the protein, several computational schemes have been used, as in ref. 19, 20. The p*K*_a values of Glu242 and His291 reported here were calculated in several models, in which different dielectric constants ϵ were assigned to protein (ϵ between 4–20), water cavities inside the protein (ϵ in the range of 10–80), the membrane ($\epsilon = 4$), and the surrounding water ($\epsilon = 80$).

The results are summarized in Fig. 3 and 4 and Tables 1–3.

3.1 The equilibrium p*K*_a values of Glu242

In Table 2, the equilibrium p*K*_a values of Glu242 are shown for two conformations of its side chain and several redox states of the metal

^{††} The four letter code refers to the redox state (R = reduced, O = oxidized) of four redox-active metal centers: Cu_A, heme *a*, heme *a*₃ and Cu_B complex, respectively. R and O refer to a total charge of the metal and its ligand. Thus, for example, Fe⁺⁴=O²⁻, Cu⁺²-OH⁻¹, Fe⁺³-OH⁻¹ are all R states, whereas Fe⁺³-H₂O, Cu⁺²-H₂O are O states.

OORO, ORRO, OORR redox states ($\epsilon_{\text{prot}} = 4$, $\epsilon_{\text{cavity}} = 20$)

A 4.2, 6.3, 21.1 $\text{H}_2\text{O}-\text{Cu}_B^{2+}$ Glu242 ⊕	C 7.3, 9.3, 23.3 $\text{H}_2\text{O}-\text{Cu}_B^{2+}$ Glu242 ⊖
B 4.0, 6.1, 20.9 $\text{H}_2\text{O}-\text{Cu}_B^{2+}$ Glu242 ⊕	D 8.7, 10.8, 24.5 $\text{H}_2\text{O}-\text{Cu}_B^{2+}$ Glu242 ⊖
E 7.7, 10.4, 12.0 $\text{H}_2\text{O}-\text{Cu}_B^{2+}$ Glu242 ⊕	F 12.0, 14.7, 15.6 $\text{H}_2\text{O}-\text{Cu}_B^{2+}$ Glu242 ⊖
8.6, 10.6, 11.5	11.2, 13.2, 12.9

Fig. 3 The mutual dependence of the p*K*_a values of His291 and Glu242 on their protonation states and conformation of Glu242 side chain, for the dielectric medium of $\epsilon_{\text{prot}} = 4$ and $\epsilon_{\text{cavity}} = 20$. See Table 3 for all other dielectric models. The sequences of numbers correspond to OORO, ORRO and OORR redox states, respectively. The p*K*_a value of His291 depends on the protonation and conformation state of Glu242: A) Glu protonated and downwards, B) Glu protonated and upwards, C) Glu deprotonated and downwards, D) Glu deprotonated and upwards. The p*K*_a of Glu242 depends on the orientation of its side chain (down/up) and the protonation state of His291: E) His protonated, F) His deprotonated.

centers. The two conformations are referred to a proton loading conformation pointing downwards, and a releasing conformation pointing upwards. In its loading conformation, Glu242 side chain

Table 2 The p*K*_a of Glu242 residue in *down* loading conformation, and in *upper* releasing conformation for the different redox states of bovine cytochrome *c* oxidase^a

Redox state ^b	p <i>K</i> _a ^c	
	Glu242 down	Glu242 up
OORO	9.0	9.4
RORO	9.2	10.0
ORRO	10.6	11.8
RRRO	10.5	11.6
OORR	9.2	9.5
RORR	9.4	9.9
ORRR	10.7	11.8
RRRR	10.9	12.0

^a The protonation state of all other residues including His291 is the equilibrium protonation state for a given redox state of metal centers.

^b The four letter code refers to the redox state (R = reduced, O = oxidized) of four redox-active metal centers: Cu_A, heme *a*, heme *a*₃ and Cu_B complex, respectively. ^c The calculations are done for $\epsilon_{\text{prot}} = 4$ and $\epsilon_{\text{cavity}} = 80$.

Table 3 The mutual dependence of the pK_a values of Glu242 and His291 on their protonation states and the conformation state of Glu242 in OORO, ORRO and OORR redox states of the enzyme^a

Dielectric medium $\epsilon_{\text{prot}}/\epsilon_{\text{cavity}}^b$	Redox state	pK_a of His291				pK_a of Glu242																			
		A		B		C		D		E		F													
		Glu prot	Glu down	Glu prot	Glu up	Glu prot	Glu up	Glu depr	Glu down	Glu prot	Glu down	Glu depr	Glu up	Glu depr	Glu down	Glu depr	Glu up								
Cont. 4	OORO ORRO OORR	15.0	18.2	35.9	14.8	17.9	35.6	20.4	23.2	39.0	21.8	24.7	40.3	18.3	21.4	23.0	17.7	21.8	24.1	22.9	26.0	25.5	24.1	28.2	29.2
4/15	OORO ORRO OORR	5.2	7.5	22.6	5.0	7.3	22.3	8.4	10.6	24.8	9.9	12.1	26.0	9.4	11.5	12.4	8.5	11.4	12.9	12.2	14.3	13.9	13.1	15.9	16.8
4/20	OORO ORRO OORR	4.2	6.3	21.1	4.0	6.1	20.9	7.3	9.3	23.3	8.7	10.8	24.5	8.6	10.6	11.5	7.7	10.4	12.0	11.2	13.2	12.9	12.0	14.7	15.6
4/80	OORO ORRO OORR	2.1	3.9	17.5	1.9	3.7	17.3	4.5	6.2	19.3	6.1	7.6	20.4	6.7	8.4	9.2	5.7	8.1	9.5	8.9	10.6	11.0	9.4	11.8	12.7
10/20	OORO ORRO OORR	7.1	8.2	17.4	7.0	8.1	17.3	8.9	9.7	18.4	9.4	10.4	19.0	4.8	5.9	6.3	5.9	7.2	7.8	6.1	7.2	7.0	7.9	9.2	9.7
20/20	OORO ORRO OORR	8.1	8.9	15.9	8.1	8.7	15.8	9.2	9.8	16.5	9.5	10.1	16.7	3.5	4.3	4.5	5.3	6.2	6.7	4.5	5.1	5.0	6.7	7.4	7.6

^a See Fig. 3 for the case of $\epsilon_{\text{prot}} = 4$, $\epsilon_{\text{cavity}} = 20$. The pK_a s of His291 and Glu242 for all other dielectric conditions can be obtained from this table. Notation of the states A–F from the table corresponds to the notation in Fig. 3A–F. ^b Calculations are done for the different dielectric conditions: in a continuum dielectric of $\epsilon = 4$ (including protein charges); and for the several cases where the dielectric of protein (ϵ_{prot}) or the solvent filled cavity (ϵ_{cavity}) was varied.

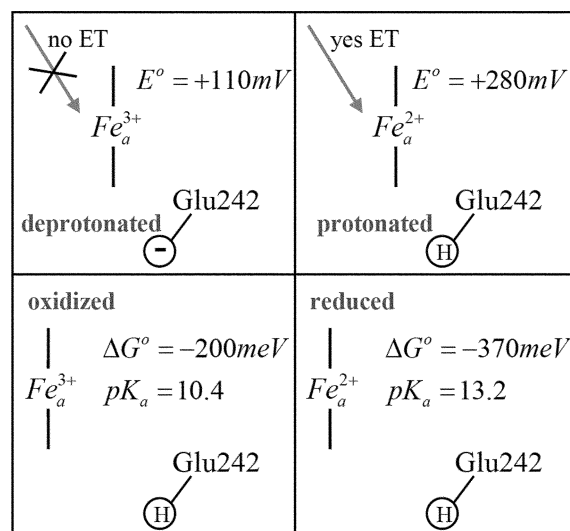


Fig. 4 The coupling of the redox state of heme *a* and protonation state of Glu242, calculated at pH = 7. The heme *a* is represented by the central Fe atom and by a line defining the porphyrin ring. The formal oxidation state shown refers to Fe atom; however, the total charge of the oxidized Fe_a -porphyrin system is +1, and for the reduced state is equal to zero.

presumably interacts with water molecules of the D-channel, which provide a proton for its reprotonation. In the upper (releasing) conformation, Glu242 is able to form a stable hydrogen bond with the chain of three water molecules leading to protonate D of heme a_3 , see Fig. 1B. The latter, in its turn, is H-bonded to His291, via an additional water molecule,^{23,30} thus providing the proton transfer pathway between Glu242 and His291, according to our model.^{15,16} In the calculations reported in Table 2, the protonation state of all other titratable residues including the His291 site is an equilibrium protonation state for a given redox state of the metal centers. For His291 this means that this residue is deprotonated if the redox state of the binuclear complex (the last two letters of the four letter notation) is RO, and protonated for the fully reduced (RR) state of the binuclear center.

From Table 2, one can see that there is no large difference in the acidity of Glu242 for different conformations of its side chain. The pK_a s in all redox states are generally somewhat smaller in the downward conformation. For both conformations, the pK_a values are higher for the states in which heme *a* is reduced. Naturally, an additional electron on heme *a* and the proton on Glu242 attract each other, increasing the pK_a value of Glu.

In Table 2, we assume that the conformational changes of Glu242 do not produce protonation changes of other titratable groups (especially of His291), and the protonation state of the enzyme is an equilibrium state, for a given redox state of metal centers. The non-equilibrium states will be discussed in the following subsections.

Comparing the equilibrium states OORO and OORR, in the latter, there is an additional electron on Cu_B , but there is also an additional proton on His291; hence, it is not surprising that the pK_a values of Glu242 in these two states are very similar (Table 1 shows that His291 and Cu_B are almost equidistant from Glu242 in both conformations).

3.2 The pK_a values in the OORO, ORRO, and OORR redox states

In this and the following subsections we analyze different redox states, and within each redox state we calculate pK_a values for His291 depending on the conformation and protonation state of Glu242; we also evaluate the pK_a values of Glu242 depending on the conformation of the Glu242 side chain and protonation state of His291. Table 3 and Fig. 3 summarize the results for the OORO, ORRO, and OORR states. Different dielectric models of the protein medium were considered. We varied two parameters—the dielectric constant of the protein matrix, ϵ_{prot} , and that of the inner water cavities, ϵ_{cavity} . We first kept $\epsilon_{\text{prot}} = 4$ constant, and gradually increased ϵ_{cavity} from 4, to 15, 20, and 80. Then, we probed the effect of increasing ϵ of the protein (4, 10, 20) while keeping $\epsilon_{\text{cavity}} = 20$ constant. The last two entries, $\epsilon_{\text{prot}}/\epsilon_{\text{cavity}} = 10/20$ and $20/20$, have been also probed, because some authors suggest^{58–60} that the protein should have much higher dielectric constant than 4, a value assumed and used in this kind of calculation for a very long time.^{51,61–66} Fig. 3 summarizes the results for a model of $\epsilon_{\text{prot}} = 4$ and $\epsilon_{\text{cavity}} = 20$. For all other dielectric conditions refer to the corresponding Table 3.

Generally, the results for homogeneous model with a dielectric of $\epsilon = 4$ shows exceedingly high pK_a s for both Glu242 and His291 in all states, see Table 3, which means they stay protonated in all redox states, and therefore this dielectric model does not make much sense. Here, the model is presented to demonstrate how much the results can change depending on the dielectric conditions.

OORO redox state

From Fig. 3 one can see that in the OORO state, when Glu242 is protonated, His291 should be deprotonated; when Glu242 is deprotonated, His likes to be protonated; and Glu itself is protonated independently of its conformation, or protonation state of His. The same conclusions are valid for $\epsilon_{\text{prot}}/\epsilon_{\text{cavity}} = 4/15$; while for $\epsilon_{\text{prot}}/\epsilon_{\text{cavity}} = 10/20$ and $20/20$, His291 is always protonated and Glu242 is always deprotonated (see Table 3). For $\epsilon_{\text{prot}}/\epsilon_{\text{cavity}} = 4/80$, the situation is somewhat different (see following discussion). Depending solely on the protonation/conformation state of the two residues their pK_a values can change by as much as 3–5 pK_a units.

Let's now look at Fig. 3D which corresponds to the second box in Fig. 2. In this state, Glu242 is in the upper conformation and has just donated a proton to the binuclear center, forming a water molecule. The pK_a of His291 at this point is 8.7. Thus, despite the presence of the chemical proton in BNC, His does not want to deprotonate. At the same time, with both protons present in BNC and on His291, the pK_a of Glu242 is 7.7 (see Fig. 3E). Thus, Glu wants to get a proton but it certainly cannot pull down the proton from the His site, because His has higher a pK_a than Glu (8.7 vs. 7.7). This remains true for all dielectric conditions involving $\epsilon_{\text{prot}} = 4$. Thus, the Glu side chain needs to swing down in order to get a proton from the D-channel. Fig. 3C shows that pK_a of His is still above 7 (protonated), when deprotonated Glu is in the downward conformation; at the same time the pK_a of Glu in that conformation with protonated His (Fig. 3E) is 8.6, which should be sufficient to pull up a proton *via* the D-channel. Once Glu gets

protonated, the pK_a of His291 drops to 4.2 (Fig. 3A), and now His can release the pumping proton on the periplasmic side of the membrane. After that, thermal fluctuations of the neutral Glu242 side chain do not affect the pK_a of His (Fig. 3A, B) much. The same mechanism of gating through conformational changes of Glu242 applies for $\epsilon_{\text{prot}}/\epsilon_{\text{cavity}} = 4/15$ (see Table 3). For the case of $\epsilon_{\text{prot}}/\epsilon_{\text{cavity}} = 4/80$, in the situation as in Fig. 3D, the pK_a of His is higher than the pK_a of Glu (6.1 vs. 5.7), thus Glu can not pull down a proton from His, but when Glu swings down, the His pK_a drops to 4.5 and the pK_a of Glu242 becomes 6.7. Once His deprotonates, the pK_a of Glu becomes 8.9 and it can receive a proton *via* the D-channel residues.

ORRO redox state

In the ORRO redox state, an additional electron is added to heme *a*, and we are interested to see how that would change the pK_a values of His291 and Glu242. Fig. 3A and 3B show that when Glu242 residue is protonated, independently on its conformation, the pK_a of His291 site is about 6; therefore it will stay deprotonated, as in the equilibrium of the OORO redox state. In addition, Figs. 3E and 3F show that Glu should have high pK_a for any conformation of its side chain and any protonation state of His291. As long as His remains deprotonated, the pK_a of Glu is above 13 for the shown dielectric conditions.

For the case of $\epsilon_{\text{prot}}/\epsilon_{\text{cavity}} = 4/80$, the situation is the same, see Table 3. His has a pK_a of 3.7–3.9 and the corresponding pK_a of Glu is 10.6–11.8 depending on the orientation of its side chain.

For $\epsilon_{\text{prot}} = 4$ and $\epsilon_{\text{cavity}} = 15$ (Table 3), after arrival of an electron and reduction of heme *a*, and with the protonated Glu242 site, the pK_a of His291 is slightly above 7. However, the pK_a of Glu is much higher, in the range of 14–16, which means that His definitely will not be able to pull out a proton from the Glu242 site. Moreover, considering that pK_a of His is just above 7, it is very unlikely that His could take a proton from any other site in its vicinity; such a site should first of all be protonated, and possess a pK_a lower than 7.5 at the same time, which is an unlikely scenario. The closest surrounding protonated sites are Arg438, Arg439 and Asp364, but our previous electrostatic calculations suggest that they have much higher pK_a values.^{15,18} Therefore, we conclude that after reduction of heme *a*, Glu242 stays protonated and it is not able to donate a proton to the His291 site, which consequently will most likely remain in the deprotonated state. However, the increased proton affinity of His291 (after reduction of heme *a*) could be a significant factor that facilitates proton transfer from Glu242 to His291, instead of that to the binuclear center, after the ET from heme *a* to Cu_B center occurs. For instance, some tendency of the His291 residue for protonation, already after arrival of an electron to heme *a*, may possibly orient the H-bonded water molecule chain to prepare the next proton transfer step toward His291 instead of the chemical proton getting to the binuclear center.²⁷

Examining the results for dielectric media of $\epsilon_{\text{prot}}/\epsilon_{\text{cavity}} = 10/20$ and $20/20$, one can see (Table 3) that His291 stays always protonated, whatever protonation/conformation state of Glu242 is. However, Glu242 pK_a values are below 7, and it should remain deprotonated in both the OORO and ORRO redox state. The latter is unlikely, which indicates the problem with the models $\epsilon_{\text{prot}}/\epsilon_{\text{cavity}} = 10/20$ and $20/20$.

OORR redox state

Upon ET to the binuclear center, and generation of the OORR redox state, the pK_a of His291 increases significantly up to 21 (see Fig. 3A and B, Table 3). At the same time, the calculated pK_a of Glu242 is between 12.9 and 15.6 (Fig. 3F). It means that His possesses a much higher pK_a than Glu, and therefore it is thermodynamically feasible for a proton translocation from Glu242 to His291 to take place. Thus, His291 gets protonated by a proton from Glu242, but deprotonated Glu242 still has a pK_a (about 12, see Fig. 3E) high enough to pull up the proton through the D-channel and get reprotonated. The results and conclusions are practically the same for all different dielectric models where $\epsilon_{\text{prot}} = 4$, see Table 3.

For dielectric models of $\epsilon_{\text{prot}}/\epsilon_{\text{cavity}} = 10/20$ and $20/20$, the obtained protonation state of His291 and Glu242 in OORR state are the same as in OORO and ORRO redox states, *i.e.* His is definitely protonated, and then Glu is deprotonated. This is in contradiction to a conventional expectation, in particular for the downward conformation of Glu, in which Glu242 is expected to receive a proton *via* the D-channel.

3.3 The effect of couplings on the pK_a s

The present DFT/electrostatic calculations demonstrate the coupling between the redox states of heme *a* and Fe_{a3} - Cu_B complex, the protonation and conformational states of Glu242, and pK_a of His291. In other words, there is an influence of the redox state of heme *a* and Cu_B on the pK_a values of His291 and Glu242 residues, as well as mutual influence of their protonation states on the pK_a of the partner. Here, we briefly summarize the results for the case of $\epsilon_{\text{prot}}/\epsilon_{\text{cavity}} = 4/15$, $4/80$, and $20/20$ (see Fig. S1 in the Electronic Supplementary Information (ESI) for further details[†]).

For $\epsilon_{\text{prot}}/\epsilon_{\text{cavity}} = 4/15$, the effect of the presence of a proton on His291 site on Glu242 residue is -4.6 (in OORO), -4.5 (in ORRO) and -3.9 pK_a units (in OORR), if Glu is in the upper conformation; the coupling is smaller, -2.8 , -2.8 and -1.5 , respectively, if Glu is in a more distant downward conformation. The coupling of the heme *a* redox state with the pK_a of Glu242 is $+2.9$ (in upper) and $+2.1$ (in down conformation). The coupling of the redox state of Cu_B to the Glu242 pK_a is $+4.4$ (in upper conformation with protonated His), $+3.7$ (with deprotonated His) and $+3.0$ (in down conformation with protonated His) and $+1.7$ (with deprotonated His). One can note that a proton on His291 and reduction of Cu_B exhibit very similar effects on the pK_a of Glu242, but only with the opposite sign. And indeed Glu242 pK_a s in the OORO(His⁻) and OORR(HisH) states are pretty much the same.

The coupling effects are about equally strong for the $\epsilon_{\text{prot}}/\epsilon_{\text{cavity}} = 4/80$ dielectric model. Thus, the coupling of the Glu242 pK_a with a proton on His291 is ranging between -3.2 to -3.7 (in upper) and -1.8 to -2.2 (in down conformation). The reduction of heme *a* produces the effect of $+2.4$ (in upper), and $+1.7$ (in down conformation). The reduction of Cu_B is coupled to the pK_a of Glu by $+3.3$ to $+3.8$ (upper) and $+2.1$ to $+2.5$ (down conformation). The extent of the effects is consistent with the interatomic distances between the corresponding groups shown in Table 1.

If the dielectric model $\epsilon_{\text{prot}}/\epsilon_{\text{cavity}} = 20/20$ is used, the coupling is very small—below 1 pK_a unit. This agrees with the interaction energies of Glu242 with PRD_{a3} , OH^- , $\text{Fe}-a$, $\text{Fe}-a_3$ and Cu_B centers, obtained in a recent study of CeO ,⁶⁰ in which the authors used an

effective dielectric constant of 20 or 40 for the protein. However, for these dielectric conditions we have shown that the pK_a values of Glu242 are too low to be realistic, and in fact are similar to those in aqueous solution ($pK_a = 4.4$),^{67,68} which is unlikely to be the case for an enzyme. It means that for such high values of ϵ for the protein, all charge–charge interactions are unrealistically decreased by the screening of the protein medium.

Fig. S2 in the ESI summarizes His291 pK_a values for different redox states and dielectric models applied in our study.[‡] From the two feasible models, $\epsilon_{\text{prot}}/\epsilon_{\text{cavity}} = 4/15$ and $4/80$, we find that the redox state of heme *a* is coupled with the protonation of His291 by about 2 pK_a units, while the coupling is much stronger to the redox state of the Cu_B center (around 14 pK_a units). Furthermore, the conformational changes of the Glu242 side chain alone have practically no effect on the pK_a of His291 if glutamic acid is protonated (neutral); but if Glu is deprotonated the effect is around 1.5 pK_a units. The maximal change of His291 pK_a due to a change of the protonation state of Glu242 is about 4–5 units.

For the case of $\epsilon_{\text{prot}}/\epsilon_{\text{cavity}} = 20/20$, the redox state of heme *a* has an effect on the His291 pK_a of only 0.6 units. The reduction of Cu_B and formation of the two-electron reduced binuclear complex affects the His site by about 7 pK_a units. The effect of Glu242 conformational changes on the pK_a of His is negligible, while the coupling of the protonation states of Glu242 to His291 pK_a is around 1 pK_a unit. His291 is protonated in all different redox, conformation and protonation states that have been examined, with its pK_a s between 8–10 for the oxidized Cu_B (OORO and ORRO) and between 15.5–16.5 for the reduced Cu_B complex (OORR state). These pK_a s become very close to those of the isolated Cu_B complex (8.6 and 13.2),¹⁹ or the binuclear complex in aqueous solution (8.9 and 14.4).²⁰ Thus, for dielectric $\epsilon_{\text{prot}}/\epsilon_{\text{cavity}} = 20/20$, the pK_a s of His291 and Glu242 exhibit the same tendency of approaching their pK_a s in water, apparently due to a large screening of the protein charges.

3.4 pK_a of Glu242 vs. E° of heme *a*

Fig. 4 displays the relationship between the protonation state and pK_a of Glu242, and the redox potential (and therefore redox state) of heme *a*. The strength of the mutual coupling between the two groups has been evaluated for the enzyme in the OORO and ORRO redox states. In the calculations, the heme *a* has been considered as an additional titratable group, which itself is redox-active and pH-independent. However, the pH dependence of its redox potential arises due to the coupling with the surrounding protonatable groups in the protein.^{69–71}

The upper part of Fig. 4 displays the dependence of the redox potential of heme *a* on the protonation state of the Glu242 residue in the downward conformation. If Glu242 is deprotonated, the calculated redox potential of heme *a* is equal to $+110$ mV, and since Cu_A and cytochrome *c* have higher redox potentials (~ 220 mV),^{72–74} the ET to heme *a* is not possible. Therefore, heme *a* remains in its oxidized state. But when Glu242 site gets protonated, the obtained redox potential of heme *a* ($+280$ mV) is higher than the E° of Cu_A and now ET can occur.

The bottom part of Fig. 4 shows that, independently of the redox state of heme *a*, the Glu242 residue possesses high pK_a values (10.4 and 13.2) and the site always wants to get a proton. The numbers shown for ΔG° (protonation free energy of Glu242)

correspond to pH = 7. The calculations are done for the dielectric model $\epsilon_{\text{prot}}/\epsilon_{\text{solvent}} = 4/80$; for the redox potential of the model compound, *bis*-histidine heme *a*, a value of -120 mV was used.⁷⁵

The strength of coupling between the two groups is found to be about 170 meV at neutral pH, which is in good qualitative agreement with the experimental measurements.^{72–74}

4. Conclusions

In this paper, we have applied DFT/continuum electrostatic calculations to study the coupling between Glu242 and His291 residues in several redox states of bovine cytochrome oxidase,³³ and for two conformations of Glu242 side chain. We have calculated the $\text{p}K_{\text{a}}$ values of His291 and Glu242 for different redox states of the metal centers, different protonation states of the two residues, and for different conformations of the Glu242 side chain. Thus, in addition to equilibrium states of the catalytic cycle, we have also covered all non-equilibrium states with respect to the protonation/conformation changes of Glu242 and His291 residues. Some of these states are transient, others are real intermediate states, while some of them are only virtual states that likely never occur.

Any calculation that includes a heterogeneous system has to deal with the problem of choosing the appropriate dielectric constants. Considering that the actual values of the dielectric constant of the protein and the inner (presumably) water-filled cavities are unknown, we examined several different dielectric models. The obtained results were then compared with experimental data, and the viability of different dielectric models in the light of the proposed proton pumping mechanism of CcO was evaluated.

The objectives of this work were to answer the following questions: How do the presence or absence of a proton on the Glu242 and/or His291 site affect the $\text{p}K_{\text{a}}$ values of the other partner? How do conformational changes of the Glu242 side chain affect the $\text{p}K_{\text{a}}$ values of the two residues in different redox states of the enzyme? What is the coupling between the redox states of heme *a* or Cu_{B} center and the protonation states of Glu242 and His291 residues? How do the redox state and redox potential of heme *a* depend on the protonation state of Glu242, and *vice versa*?

Here it is particularly interesting to compare the obtained $\text{p}K_{\text{a}}$ values of Glu242 in different redox states of the enzyme with the results of a recent work,³⁴ which suggests that the Glu242 residue might be deprotonated in some of the states in the catalytic cycle. Several other studies, based on the pH-dependent proton transfer (PT) rates and FTIR measurements, suggest that Glu242 is protonated at pH 7 with an apparent $\text{p}K_{\text{a}} \geq 9$.^{35–40} An interesting model of reprotonation of Glu242 was published recently by Xu and Voth.⁷⁶

Our calculations show that in a broad range of $\epsilon_{\text{prot}} = 4–8$ and $\epsilon_{\text{cavity}} = 4–80$, the $\text{p}K_{\text{a}}$ s of Glu242 are above 7 for all redox states, and therefore at equilibrium it should be always protonated. The best agreement with the available experimental data is obtained for $\epsilon_{\text{prot}} = 4$ and $\epsilon_{\text{cavity}} = 80$, however, dielectric models ($\epsilon_{\text{prot}} = 4$, $\epsilon_{\text{cavity}} = 15$ or 20) also give reasonable agreement.

Within these dielectric models, the only case when Glu242 residue was found to be deprotonated is for the OORO redox state and $\epsilon_{\text{prot}}/\epsilon_{\text{cavity}} = 4/80$. Here, Glu242 can remain deprotonated, after it delivers a chemical proton to the binuclear center to form a water molecule, and before His291 site gets rid of its own H δ 1

proton, provided that Glu242 is somehow trapped in its upward conformation. For the case ($\epsilon_{\text{prot}}/\epsilon_{\text{cavity}} = 4/80$), Glu has a $\text{p}K_{\text{a}}$ of 5.7 in the upper conformation, prior to the ejection of a proton from the His site. Even in the downward conformation its $\text{p}K_{\text{a}}$ is low (6.7), if His still keeps the proton. Thus, according to the present calculation, unless the release of the proton from His291 is somehow blocked and Glu stays in the upper conformation, this group remains protonated at equilibrium.

Interestingly, in agreement with present calculations is our previous finding that the OH⁻ ligand to Cu_B has a computed $\text{p}K_{\text{a}}$ of 8.5 to 9.6 in the OORO redox state of the enzyme prior to the pumping event, *i.e.* when His291 is still protonated.²⁰ Thus, OH⁻ ligand possesses a higher $\text{p}K_{\text{a}}$ than the Glu242 residue (5.7–6.7), and therefore it can pull out H⁺ from the Glu site, as our model assumes.¹⁶ The ejection of the proton from the His291 site can only further increase the $\text{p}K_{\text{a}}$ of the Cu_B-OH⁻ ligand, which therefore will remain protonated, *i.e.* as H₂O.

Other dielectric models, $\epsilon_{\text{prot}} = 10$ and $\epsilon_{\text{cavity}} = 10$ or 20, give too low values of $\text{p}K_{\text{a}}$ for Glu242 (below 7) in all redox states, which do not agree with experiments. At the same time the His291 site possesses $\text{p}K_{\text{a}}$ s higher than 7, which means that it always remains protonated. As already discussed, in these two models the gating through the conformational changes of the Glu side chain is not possible, because in the OORO redox state even an additional proton on Glu is not enough to push out a proton from His site. Also, the $\text{p}K_{\text{a}}$ s of Glu in the downward conformation are so low that Glu cannot get reprotonated *via* the D-channel. Therefore, the results of these two dielectric models do not fit to either the proton pumping mechanism that we proposed,^{15,16} or the results of the experimental measurements.^{35–40}

It should be remembered, that the correct dielectric description of the protein is still an unsettled question, and the function of His291 as a proton pump has not been confirmed, or refuted by the experiment; moreover, some calculations do not support our proposal that His291 changes its protonation state during the enzyme cycle.⁷⁷ (The latter calculation, however, did not have a correct geometry optimization of one of the protonation states, and has other serious drawbacks, therefore we believe the conclusions of ref. 77 are ill supported, see our Comment to JPC, ref. 78.)

The main findings of this work can be summarized as follows. The results of this paper support our earlier proposed proton pumping mechanism of CcO.¹⁶ The $\text{p}K_{\text{a}}$ of His291 depends on the redox state of the enzyme. His291 wants to be protonated in the OORR redox state, and deprotonated in the OORO state. In the OORR state, Glu242 also possesses a $\text{p}K_{\text{a}} > 7$, but lower than the $\text{p}K_{\text{a}}$ of His291. Therefore, Glu can transfer a proton to a His-site, but afterward it should quickly get reprotonated, unless it is somehow trapped in the upper conformation.

In the OORO redox state, we find that after donating a proton to the OH⁻ ligand in BNC, Glu242 needs to be reprotonated before His291 can release a proton, and the pumping occurs. Thus, the reprotonation of Glu can be said to displace an H⁺ from the PLS. This result is in agreement with a recent work of Brzezinski and coworkers.⁷⁹ Moreover, our calculations suggest that a subtle mechanism of gating through conformational changes in the Glu side chain may be employed by the enzyme. Namely, in the OORO state with deprotonated Glu in the upper conformation, the proton-pump site His291 still remains protonated, and has a

pK_a higher than that of Glu242. In its upward conformation Glu also has a $pK_a > 7$, but since it cannot get a proton from any residue from the upper side, the only way for it to get protonated is to swing down. This will simultaneously decrease the proton affinity of His site and further increase the pK_a of the Glu site. In the downward conformation, the Glu residue will re-establish the H-bond connectivity with the D-channel, and will then quickly get reprotonated. The reprotonation of Glu ultimately decreases the pK_a of the His291 site, which will release the pumped proton into the cytosolic side (P-side) of the membrane.

In the *equilibrium* stable states of the catalytic cycle that we examined, it is most likely that Glu is never deprotonated. Of course, since Glu242 residue is the proton donor of both chemical and pump protons, in some of the *transient* states Glu gets temporarily deprotonated, after it transfers a proton to an acceptor group with a higher pK_a (His291 or OH^-). However, in all of these intermediate (transient) states, the obtained pK_a s of Glu are high enough to pull up a proton from the D-channel and get reprotonated once again.

Additionally, we have explored the mutual coupling between the protonation state and pK_a of Glu242 and the redox state and potential of heme *a*. We find that the protonation state of Glu is independent of the redox state of heme *a*, though its pK_a value is sensitive to the redox changes of the system. On the other hand, the reduction of heme *a* is only possible if the Glu242 site is protonated. The strength of the coupling between the two groups is about 170 meV at neutral pH, which is in good agreement with the experimental measurements.⁷²⁻⁷⁴

Acknowledgements

We wish to thank Dr. Jason Quenneville for his helpful input of electronic structure calculations. This work has been supported by the NSF grant and a research grant from the NIH (GM54052).

References

- G. T. Babcock and M. Wikström, Oxygen activation and the conservation of energy in cell respiration, *Nature*, 1992, **356**, 301–309.
- S. Ferguson-Miller and G. T. Babcock, Heme-copper oxidase, *Chem. Rev.*, 1996, **7**, 2889–2907.
- M. Wikström, Proton translocation by bacteriorhodopsin and heme-copper oxidases, *Curr. Opin. Struct. Biol.*, 1998, **8**, 480–488.
- R. B. Gennis, How does cytochrome oxidase pump protons?, *Proc. Natl. Acad. Sci. U. S. A.*, 1998, **95**, 12747–12749.
- H. Michel, J. Behr, A. Harrenga and A. Kannt, Cytochrome c oxidase: Structure and spectroscopy, *Annu. Rev. Biophys. Biomol. Struct.*, 1998, **27**, 329–356.
- H. Michel, Cytochrome c oxidase: Catalytic cycle and mechanism of proton pumping - a discussion, *Biochemistry*, 1999, **38**, 15129–15140.
- D. Zaslavsky and R. B. Gennis, Proton pumping by cytochrome oxidase: progress, problems and postulates, *Biochim. Biophys. Acta*, 2000, **1458**, 164–179.
- M. Wikström, Proton translocation by cytochrome c oxidase: a rejoinder to recent criticism, *Biochemistry*, 2000, **39**, 3515–3519.
- M. Wikström, A. Jasaitis, C. Backgren, A. Puustinen and M. I. Verkhovskiy, The role of the D- and K-pathways of proton transfer in the function of the haem-copper oxidases, *Biochim. Biophys. Acta*, 2000, **1459**, 514–520.
- S. Han, S. Takahashi and D. L. Rousseau, Time dependence of the catalytic intermediates in cytochrome c oxidase, *J. Biol. Chem.*, 2000, **275**, 1910–1919.
- D. A. Mills, L. Florens, C. Hiser, J. Qian and S. Ferguson-Miller, Where is “outside” in cytochrome c oxidase and how and when do protons get there?, *Biochim. Biophys. Acta*, 2000, **1458**, 180–187.

- P. Brzezinski, Redox-driven membrane-bound proton pumps, *Trends Biochem. Sci.*, 2004, **29**, 380–387.
- R. B. Gennis, Coupled proton and electron transfer reactions in cytochrome oxidase, *Front. Biosci.*, 2004, **9**, 581–591.
- M. Wikström, Cytochrome c oxidase: 25 years of the elusive proton pump., *Biochim. Biophys. Acta*, 2004, **1655**, 241–247.
- D. M. Popovic and A. A. Stuchebrukhov, Electrostatic study of proton pumping mechanism of bovine heart cytochrome c oxidase, *J. Am. Chem. Soc.*, 2004, **126**, 1858–1871.
- D. M. Popovic and A. A. Stuchebrukhov, Proton pumping mechanism and catalytic cycle of cytochrome c oxidase: Coulomb pump model with kinetic gating, *FEBS Lett.*, 2004, **566**, 126–130.
- J. Quenneville, D. M. Popovic and A. A. Stuchebrukhov, Redox-dependent pK_a of CuB histidine ligand in cytochrome c oxidase, *J. Phys. Chem. B*, 2004, **108**, 18383–18389.
- D. M. Popovic and A. A. Stuchebrukhov, Proton exit channels in bovine cytochrome c oxidase, *J. Phys. Chem. B*, 2005, **109**, 1999–2006.
- D. M. Popovic, J. Quenneville and A. A. Stuchebrukhov, DFT/electrostatic calculations of pK_a values in cytochrome c oxidase, *J. Phys. Chem. B*, 2005, **109**, 3616–3626.
- J. Quenneville, D. M. Popovic and A. A. Stuchebrukhov, Combined DFT and Electrostatics Study of the Proton Pumping Mechanism in Cytochrome c Oxidase, *Biochim. Biophys. Acta*, 2006, in press.
- M. L. Verkhovskaya, A. Garcia-Horsman, A. Puustinen, J.-L. Rigaud, J. E. Morgan, M. I. Verkhovskiy and M. Wikström, Glutamic acid 286 in subunit I of cytochrome bo3 is involved in proton translocation, *Proc. Natl. Acad. Sci. U. S. A.*, 1997, **94**, 10128–10131.
- P. Adelroth, M. S. Ek, D. M. Mitchell, R. B. Gennis and P. Brzezinski, Glutamate 286 in cytochrome aa3 from *Rhodobacter sphaeroides* is involved in proton uptake during the reaction of the fully-reduced enzyme with dioxygen, *Biochemistry*, 1997, **36**, 13824–13829.
- M. Svensson-Ek, J. Abramson, G. Larsson, S. Tornroth, P. Brzezinski and S. Iwata, The X-ray crystal structures of wild-type and EQ(I-286) mutant cytochrome c oxidases from *Rhodobacter Sphaeroides*, *J. Mol. Biol.*, 2002, **321**, 329–335.
- A. S. Pawate, J. Morgan, A. Namslauer, D. Mills, P. Brzezinski, S. Ferguson-Miller and R. B. Gennis, A mutation in subunit I of cytochrome oxidase from *Rhodobacter sphaeroides* results in an increase in steady-state activity but completely eliminates proton pumping, *Biochemistry*, 2002, **41**, 13417–13423.
- X. Zheng, D. M. Medvedev, J. Swanson and A. A. Stuchebrukhov, Computer simulation of water in cytochrome c oxidase, *Biochim. Biophys. Acta*, 2003, **1557**, 99–107.
- M. Tashiro and A. A. Stuchebrukhov, Thermodynamic properties of internal water molecules in the hydrophobic cavity around the catalytic center of cytochrome c oxidase, *J. Phys. Chem. B*, 2005, **109**, 1015–1022.
- M. Wikström, M. I. Verkhovskiy and G. Hummer, Water-gated mechanism of proton translocation by cytochrome c oxidase, *Biochim. Biophys. Acta*, 2003, **1604**, 61–65.
- I. Hofacker and K. Schulten, Oxygen and proton pathways in cytochrome c oxidase, *Proteins*, 1998, **30**, 100–107.
- R. Pomes, G. Hummer and M. Wikström, Structure and dynamics of a proton shuttle in cytochrome c oxidase, *Biochim. Biophys. Acta*, 1998, **1365**, 255–260.
- C. Ostermeier, A. Harrenga, U. Ermler and H. Michel, Structure at 2.7 Å resolution of the *Paracoccus denitrificans* two-subunit cytochrome c oxidase complexed with an antibody Fv fragment, *Proc. Natl. Acad. Sci. U. S. A.*, 1997, **94**, 10547–10553.
- T. Tsukahara, K. Shimokata, Y. Katayama, H. Shimada, K. Muramoto, H. Aoyama, M. Mochizuki, K. Shinzawa-Itoh, E. Yamashita, M. Yao, Y. Ishimura and S. Yoshikawa, The low-spin heme of cytochrome c oxidase as the driving element of the proton-pumping process, *Proc. Natl. Acad. Sci. U. S. A.*, 2003, **100**, 15304–15309.
- R. B. Gennis and P. Brzezinski, The X-ray crystal structures of CcO from *Rhodobacter sphaeroides*-wild type and EQ(I-286) mutant at pH 10, personal communication.
- S. Yoshikawa, K. Shinzawa-Itoh, R. Nakashima, R. Yaono, E. Yamashita, N. Inoue, M. Yao, M. J. Fei, C. P. Libeu, T. Mizushima, H. Yamaguchi, T. Tomizaki and T. Tsukahara, Redox-coupled structural changes in bovine heart cytochrome c oxidase, *Science*, 1998, **280**, 1723–1729.
- R. M. Nyquist, D. Heitbrink, C. Bolwien, R. B. Gennis and J. Heberle, Direct observation of protonation reactions during the catalytic cycle

- of cytochrome oxidase, *Proc. Natl. Acad. Sci. U. S. A.*, 2003, **100**, 8715–8720.
- 35 M. Lübbers and K. Gerwert, Redox difference spectroscopy using caged electrons reveals contributions of carboxyl groups to the catalytic mechanism of heme-copper oxidases, *FEBS Lett.*, 1996, **397**, 303–307.
 - 36 P. Hellwig, B. Rost, U. Kaiser, C. Ostermeier, H. Michel and W. Mantele, Carboxyl group protonation upon reduction of the Paracoccus denitrificans cytochrome c oxidase: direct evidence by FTIR spectroscopy, *FEBS Lett.*, 1996, **385**, 53–57.
 - 37 A. Puustinen, J. A. Bailey, R. B. Dyer, S. L. Mecklenberg and M. Wikström, Fourier transform infrared evidence for connectivity between CuB and glutamic acid 286 in cytochrome bo₃ from Escherichia coli, *Biochemistry*, 1997, **36**, 13195–13200.
 - 38 P. Hellwig, J. Behr, C. Ostermeier, O.-M. H. Richter, U. Pfützner, A. Odenwald, B. Ludwig, H. Michel and W. Mantele, Involvement of glutamic acid 278 in the redox reaction of the cytochrome c oxidase from Paracoccus denitrificans investigated by FT-IR spectroscopy, *Biochemistry*, 1998, **37**, 7390–7399.
 - 39 M. Lübbers, A. Prutsch, B. Mamat and K. Gerwert, Electron transfer induces side-chain conformational changes of glutamate-286 from cytochrome bo₃, *Biochemistry*, 1999, **38**, 2048–2056.
 - 40 A. Namslaufer, A. Aagaard, A. Katsonouri and P. Brzezinski, Redox-coupled proton translocation in biological systems: Proton shuttling in cytochrome c oxidase, *Biochemistry*, 2003, **42**, 1488–1498.
 - 41 Jaguar 5.5, Schrödinger, L. L. C., Portland, OR, 1991–2003.
 - 42 D. Bashford, An object-oriented programming suite for electrostatic effects in biological molecules, in *Scientific Computing in Object-Oriented Parallel Environments*, ed. Y. Ishikawa, R. R. Oldehoeft, J. V. W. Reyniers and M. Tholburn, Springer, Berlin, 1997, pp. 233–240.
 - 43 B. Rabenstein. Karlsruhe online manual: <http://lie.chemie.fu-berlin/karlsberg/ed.1999>.
 - 44 K. Kohn and L. J. Sham, Self-consistent equations including exchange and correlation effects., *Phys. Rev.*, 1965, **140**, A1133–1136.
 - 45 A. D. Becke, Density-functional thermochemistry. III. The role of exact exchange., *J. Chem. Phys.*, 1993, **98**, 5648–5652.
 - 46 P. J. Hay and W. R. Wadt, Ab initio effective core potentials for molecular calculations. Potentials for K to Au including the outermost core orbitals., *J. Chem. Phys.*, 1985, **82**, 299–310.
 - 47 D. J. Tannor, B. Marten, R. Marphy, R. A. Friesner, D. Sitkoff, A. Nicholls, M. Ringnalda, W. A. Goddard, III and B. Honig, Accurate first principles calculation of molecular charge distributions and solvation energies from ab initio quantum mechanics and continuum dielectric theory, *J. Am. Chem. Soc.*, 1994, **116**, 11875–11880.
 - 48 J. L. Chen, L. Noodleman, D. A. Case and D. Bashford, Incorporating solvation effects into density functional electronic structure calculations, *J. Phys. Chem.*, 1994, **98**, 11059–11068.
 - 49 J. M. Mouesca, J. L. Chen, L. Noodleman, D. Bashford and D. A. Case, Density functional/Poisson-Boltzmann calculations of redox potentials for iron-sulfur clusters, *J. Am. Chem. Soc.*, 1994, **116**, 11898–11914.
 - 50 J. Li, C. L. Fischer, J. L. Chen, D. Bashford and L. Noodleman, Calculation of redox potentials and pK_a values of hydrated transition metal cations by a combined density functional and continuum dielectric theory, *J. Phys. Chem.*, 1996, **96**, 2855–2866.
 - 51 J. Li, M. R. Nelson, C. Y. Peng, D. Bashford and L. Noodleman, Incorporating protein environments in density functional theory: A self-consistent reaction field calculation of redox potentials of [2Fe2S] clusters in ferredoxin and phthalate dioxygenase reductase, *J. Phys. Chem. A*, 1998, **102**, 6311–6324.
 - 52 J. Li, C. L. Fisher, R. Konecny, D. Bashford and L. Noodleman, Density functional and electrostatic calculations of manganese superoxide dismutase active site complexes in protein environments, *Inorg. Chem.*, 1999, **38**, 929–939.
 - 53 G. M. Ullmann, L. Noodleman and D. A. Case, Density functional calculation of pK_a values and redox potentials in the bovine Rieske iron-sulfur protein, *J. Biol. Inorg. Chem.*, 2002, **7**, 632–639.
 - 54 R. Ditchfield, W. J. Hehre and J. A. Pople, Self-consistent molecular-orbital methods. IX. An extended Gaussian-type basis for molecular-orbital studies of organic molecules, *J. Chem. Phys.*, 1971, **54**, 724–728.
 - 55 W. J. Hehre, R. Ditchfield and J. A. Pople, Self-consistent molecular orbital methods. XII. Further extensions of Gaussian-type basis sets for use in molecular orbital studies of organic molecules, *J. Chem. Phys.*, 1972, **56**, 2257–2261.
 - 56 W. J. Hehre and J. A. Pople, Self-consistent molecular orbital methods. XIII. An extended Gaussian-type basis for boron, *J. Chem. Phys.*, 1972, **56**, 4233–4234.
 - 57 P. C. Hariharan and J. A. Pople, The influence of polarization functions on molecular orbital hydrogenation energies, *Theor. Chim. Acta*, 1973, **28**, 213–222.
 - 58 C. N. Schutz and A. Warshel, What are the dielectric “constants” of proteins and how to validate electrostatic models, *Proteins*, 2001, **44**, 400–417.
 - 59 M. Wojciechowski, T. Grycuk, J. M. Antosiewicz and B. Lesyng, Prediction of secondary ionization of the phosphate group in phosphotyrosine peptides, *Biophys. J.*, 2003, **84**, 750–756.
 - 60 M. H. M. Olsson, P. K. Sharma and A. Warshel, Simulating redox coupled proton transfer in cytochrome c oxidase: Looking for the proton bottleneck, *FEBS Lett.*, 2005, **579**, 2026–2034.
 - 61 K. Sharp and B. Honig, Electrostatic interactions in macromolecules: Theory and applications., *Annu. Rev. Biophys. Biophys. Chem.*, 1990, **19**, 301–332.
 - 62 D. Bashford, D. A. Case, C. Dalvit, L. Tennant and P. E. Wright, Electrostatic calculations of side-chain pK_a values in myoglobin and comparison with NMR data for histidines, *Biochemistry*, 1993, **32**, 8045–8056.
 - 63 T. Simonson and D. Perahia, Internal and interfacial dielectric properties of cytochrome c from molecular dynamics in aqueous solution, *Proc. Natl. Acad. Sci. U. S. A.*, 1995, **92**, 1082–1086.
 - 64 T. Simonson and C. L. Brooks, Charge separation and the dielectric constant of proteins: Insights from molecular dynamics, *J. Am. Chem. Soc.*, 1996, **118**, 8452–8458.
 - 65 A. Warshel and A. Papazyan, Electrostatic effects in macromolecules: Fundamental concepts and practical modeling, *Curr. Opin. Struct. Biol.*, 1998, **8**, 211–217.
 - 66 A. Onufriev, A. Smondyrev and D. Bashford, Affinity changes driving unidirectional proton transport in the bacteriorhodopsin photocycle, *J. Mol. Biol.*, 2003, **332**, 1183–1193.
 - 67 Y. Nozaki and C. Tanford, Intrinsic dissociation constants of aspartyl and glutamyl carboxyl groups, *J. Biol. Chem.*, 1967, **242**, 4731.
 - 68 C. Tanford and R. Roxby, Interpretation of protein titration curves. Application to lysozyme, *Biochemistry*, 1972, **11**, 2192–2198.
 - 69 D. M. Popovic, S. D. Zaric, B. Rabenstein and E. W. Knapp, Artificial cytochrome b: Computer modeling and evaluation of redox potentials, *J. Am. Chem. Soc.*, 2001, **123**, 6040–6053.
 - 70 D. M. Popovic, A. Zmiric, S. D. Zaric and E. W. Knapp, Energetics of radical transfer in DNA photolyase, *J. Am. Chem. Soc.*, 2002, **124**, 3775–3782.
 - 71 A. M. Baptista, P. J. Martel and C. M. Soares, Simulation of electron-proton coupling with a Monte Carlo method: Application to cytochrome c₃ using continuum electrostatics, *Biophys. J.*, 1999, **76**, 2978–2998.
 - 72 M. I. Verkhovskiy, J. E. Morgan and M. Wikström, Control of electron delivery to the oxygen reduction site of cytochrome c oxidase: A role for protons, *Biochemistry*, 1995, **34**, 7483–7491.
 - 73 A. V. Xavier, A mechano-chemical model for energy transduction in cytochrome c oxidase: the work of a Maxwell’s god, *FEBS Lett.*, 2002, **532**, 261–266.
 - 74 A. V. Xavier, Thermodynamic and choreographic constraints for energy transduction by cytochrome c oxidase, *Biochim. Biophys. Acta*, 2004, **1658**, 23–30.
 - 75 B. R. Gibney, Y. Isogai, F. Rabanal, K. S. Reddy, A. M. Grosset, C. C. Moser and P. L. Dutton, Self-assembly of heme a and heme b in a designed four-helix bundle: Implications for a cytochrome c oxidase maquette, *Biochemistry*, 2000, **39**, 11041–11049.
 - 76 J. Xu and G. A. Voth, Computer simulation of explicit proton translocation in cytochrome c oxidase: The D-pathway, *Proc. Natl. Acad. Sci. U. S. A.*, 2005, **102**, 6795–6800.
 - 77 E. Fadda, N. Chakrabarti and R. Pomes, Acidity of a Cu-bound histidine in the binuclear center of cytochrome c oxidase, *J. Phys. Chem. B*, 2005, **109**, 22629–22640.
 - 78 A. A. Stuchebrukhov and D. M. Popovic, Comment on “Acidity of a Cu-bound histidine in the binuclear center of cytochrome c oxidase” by E. Fadda, N. Chakrabarti, R. Pomes, *J. Phys. Chem. B*, 2006, in press.
 - 79 K. Faxen, G. Gilderson, P. Ådelroth and P. Brzezinski, A mechanistic principle for proton pumping by cytochrome c oxidase, *Nature*, 2005, **437**, 286–289.